

A practical framework for analyzing high-dimensional QKD setups

Florian Kanitschar^{1,2,*} and Marcus Huber¹

¹*Vienna Center for Quantum Science and Technology (VCQ), Atominstitut,
Technische Universität Wien, Stadionallee 2, 1020 Vienna, Austria*

²*AIT Austrian Institute of Technology, Center for Digital Safety&Security, Giefinggasse 4, 1210 Vienna, Austria*

(Dated: June 14, 2024)

High-dimensional (HD) entanglement promises both enhanced key rates and overcoming obstacles faced by modern-day quantum communication. However, modern convex optimization-based security arguments are limited by computational constraints; thus, accessible dimensions are far exceeded by progress in HD photonics, bringing forth a need for efficient methods to compute key rates for large encoding dimensions. In response to this problem, we present a flexible analytic framework facilitated by the dual of a semi-definite program and diagonalizing operators inspired by entanglement-witness theory, enabling the efficient computation of key rates in high-dimensional systems. To facilitate the latter, we show how matrix completion techniques can be incorporated to effectively yield improved, computable bounds on the key rate in paradigmatic high-dimensional systems of time- or frequency-bin entangled photons and beyond.

Introduction.— Quantum key distribution is one of the most mature quantum technologies, yet still faces fundamental challenges to be overcome for long-distance applications. While the exponential loss in optical fibers can be overcome by moving to free space, other issues such as low key rate and, in particular, low noise tolerance prevail. The latter limits free-space and satellite-based realizations to nighttime operations, severely reducing up-time and a significant impediment to practical feasibility. Recent works have shown efforts to extend operation times gradually, mainly by experimental adaptations [1–7]. However, this did not turn out sufficient to close this gap and hints that additional developments from the theoretical and protocol side are required.

Elaborate forms of entanglement beyond qubit entanglement are a promising platform to address this issue. High-dimensional (HD) entanglement [5, 6, 8–13], besides naturally increasing the key rate per signal, has proven to enhance background noise-resistance [14] in entanglement-distribution tasks. States that are entangled in high dimensions can be produced in labs in various degrees of freedom, among others in the temporal domain [15–17], the frequency domain [18], and in the form orbital angular momentum entanglement [19], as well as in combinations of those, leading to hyperentangled states [20, 21]. However, from the theoretical side, the available tools for calculating secure key rates in high-dimensional quantum systems are rather limited. On one hand, there are methods [22, 23] requiring Alice and Bob to measure between two and $d + 1$ mutually unbiased bases, which is already practically infeasible in low to medium dimensions. On the other hand, numerical methods [24–27] can avoid impractical measurements but rely on computationally very expensive and RAM-intensive convex optimization procedures. These demands are particularly challenging for high-dimensional problems, limiting the

practical dimensionality to the low teens with state-of-the-art hardware [25], while cutoffs [28–30] or established reduction methods [31, 32] known from DM CVQKD cannot be applied for HD QKD protocols. At the same time, recent progress in high-dimensional photonics exceeds those limitations by far and brings forth the need for methods to compute secure key rates in the regime of significantly larger encoding dimensions.

Our work addresses this issue by introducing a framework for analyzing practical High-Dimensional QKD setups without relying on infeasible measurements or computationally expensive convex optimization methods. We rewrite the Devetak-Winter formula [33] for the secure key rate as a semi-definite program (SDP) constrained by linear functions of certain observables that can be derived from the actual measurements inspired by entanglement witnesses. Instead of solving this SDP directly, we derive its dual, which is guaranteed to lower bound the primal SDP, hence the secure key rate. We show that the dual problem can be simplified and rewritten so that it boils down to finding the largest eigenvalue of a parametrized matrix and solving a scalar-valued optimization problem constrained by linear functions of the largest eigenvalue. Additionally, we introduce a method that allows us to conveniently express or at least upper-bound those largest eigenvalues for a broad class of relevant matrices. Then, the resulting optimization problem can be solved using either Lagrange’s or numerical methods. The reduction to a dimension-independent optimization problem (besides the eigenvalue-calculation) significantly decreases the computational demands of the key rate calculation task while still yielding reliable lower bounds. The choice of the operators used can be tailored to a) meet the requirements of the concrete physical measurement setup and/or b) simplify the expression for the largest eigenvalue, hence the whole optimization problem. Our method accommodates subspace postselection, which is known to improve key rates further, particularly in very noisy scenarios [23], and we demonstrate how matrix completion techniques can be used to extend the

* florian.kanitschar@outlook.com

range of possible observables used further by providing bounds on their expectations. Finally, we illustrate our method and calculate asymptotic secure key rates for a high-dimensional temporal entanglement setup analyzed in [25].

Protocol.— We analyze a general high-dimensional QKD protocol, comprised of the following steps.

1.) State Generation. A photon source distributes entangled quantum states ρ_{AB} to Alice and Bob.

2.) Measurement. Alice and Bob randomly and independently decide to measure either in their computational bases $\{A_1^x\}_{x=0}^{d-1}, \{B_1^y\}_{x=0}^{d-1}$ or in one of the test bases $\{A_2^x\}_{x=0}^{d-1}, \{B_2^y\}_{x=0}^{d-1}$ and record their outcomes in their respective registers.

Steps 1.) and 2.) are repeated many times.

3.) Sifting. Alice and Bob use the classical authenticated channel to communicate their measurement choice to each other and may discard certain results. They also may choose to perform subspace postselection.

4.) Parameter Estimation. The communicating parties disclose some of their measurement results over the public channel to estimate the correlations between their bit-strings.

5.) Error-Correction & Privacy Amplification. Finally, on the remaining rounds, Alice and Bob perform error-correction and privacy amplification to reconcile their raw keys X and Y and decouple them from Eve.

Key Rate Calculation.— As in the asymptotic regime collective i.i.d. attacks are known to be essentially optimal [34], worst-case, after protocol execution, Eve holds a purification ρ_{ABE} of Alice's and Bob's shared state ρ_{AB} . Let us denote the map representing the (unknown) quantum channel by \mathcal{E}^{ch} , the map describing Alice's and Bob's measurements by $\mathcal{E}^{\text{meas}}$ and the map describing the classical postprocessing steps by \mathcal{E}^{PP} . Summarizing the action of all those maps by $\mathcal{E} := \mathcal{E}^{\text{PP}} \circ \mathcal{E}^{\text{meas}} \circ \mathcal{E}^{\text{ch}}$, the state after protocol execution reads $\sigma_{XYE'} := \mathcal{E}(\rho_{ABE})$. The following does not explicitly assume that subspace postselection is performed but generally treats a QKD protocol in dimension d . However, according to [23, Theorem 1], the asymptotic key rates for the protocol including subspace postselection, employing l subspaces of dimension D , (s.t. $d = l \times D$), are simply given by the weighted average of l full space protocols of dimension D , $K \geq \sum_{m=0}^{\ell-1} P(M = m) K_m$ such that we can easily relate them to each other by replacing d by D and building the weighted sum. Here, $P(M = m)$ is the probability that Alice and Bob obtain an outcome in the same subspace and K_m is the key rate obtained from this subspace. The Devetak-Winter formula [33] $R^\infty = H(X|E) - H(X|Y)$ quantifies the asymptotic key rate of a QKD protocol as the difference between Eve's lack of knowledge about Alice's bitstring X and the amount of information Alice needs to communicate to Bob in order to reconcile their keys X and Y . Since the second term is purely classical and can be directly calculated from Alice's and Bob's data, we focus on the first

term which can be lower bounded by the min-entropy, $H(X|E)_\rho \geq H_{\min}(X|E)_\rho$. The latter is connected to the logarithm of Eve's average probability of guessing Alice's key string correctly, $H_{\min}(X|E)_\rho = -\log_2(p_{\text{guess}})$. Thus, in order to lower bound the asymptotic secure key rate, it suffices to find a way of calculating Eve's average guessing probability. We can formulate (see, for example, Ref. [23]) the average guessing probability as an optimization problem, where we maximize the probability that Eve guesses Alice's measurement outcome correctly over all purifications ρ_{ABE} (which we assume to be held by Eve) of Alice's and Bob's shared state ρ_{AB} and over all possible measurements $\{E^e\}_e$ Eve might carry out, constrained by physical requirements and Alice's and Bob's observations.

$$\begin{aligned}
 p_{\text{guess}} &= \max_{\rho_{ABE}, \{E^\ell\}_{\ell=0}^{d-1}} \sum_{\ell, y} \text{Tr} [\rho_{ABE} A_1^\ell \otimes B_1^k \otimes E^\ell] \\
 \text{s.t.} & \\
 &\sum_{\ell} E^\ell = \mathbb{1}, \\
 &\text{Tr} [\rho_{ABE}] = 1, \\
 &w_k = \text{Tr} \left[\left(\hat{W}_k^{(e)} \otimes \mathbb{1}_E \right) \rho_{ABE} \right], \\
 &w_j^L \leq \text{Tr} \left[\left(\hat{W}_j^{(i)} \otimes \mathbb{1}_E \right) \rho_{ABE} \right] \leq w_j^U, \\
 &E^\ell \geq 0, \\
 &\rho_{ABE} \geq 0,
 \end{aligned} \tag{1}$$

for $k \in \{1, \dots, N_{eW}\}$, $j \in \{1, \dots, N_{iW}\}$ and $\ell \in \{0, \dots, d-1\}$. While A_1 and B_1 denote Alice's and Bob's computational basis, the operators $\hat{W}_k^{(e)}$ are observables with expectations w_k known with equality and $\hat{W}_j^{(i)}$ are observables where we can only find upper and/or lower bounds w_j^U and w_j^L for its expectations. As we derive in the Appendix, the dual of this SDP can be brought into the form

$$\begin{aligned}
 \min y_0 + \sum_{k=1}^{N_{eW}} y_k w_k + \sum_{j=1}^{N_{iW}} (z_j^U w_j^U - z_j^L w_j^L) \\
 \text{s.t.} \\
 y_0 \geq \lambda_{\max}(M_\ell) \quad \forall \ell = 0, \dots, d-1 \\
 z_j^L, z_j^U \geq 0 \quad \forall j = 1, \dots, N_{iW} \\
 y_k \in \mathbb{R} \quad \forall k = 0, \dots, N_{eW},
 \end{aligned} \tag{2}$$

where $\lambda_{\max}(M_\ell)$ denotes the largest eigenvalue of $M_\ell := |\ell\rangle\langle\ell| \otimes \mathbb{1}_d - \sum_{k=1}^{N_{eW}} y_k \bar{W}_k^{(e)} - \sum_{j=1}^{N_{iW}} (z_j^U - z_j^L) \bar{W}_j^{(i)}$. Due to the SDP duality theory, every solution of this dual problem is a valid upper bound for the guessing probability, hence giving rise to a valid lower bound on the secure key rate. By this procedure, we reduced the task of solving a computationally expensive optimization problem that turns out to be computationally infeasible already for medium dimensions to finding the largest eigenvalue of

a matrix and solving a much simpler optimization problem. The matrix M_ℓ is a function of the observables chosen to formulate the initial optimization problem for the guessing probability. Thus, obviously, the choice of the observables heavily influences both the structure of the optimization problem, hence difficulty, and the final result, hence the obtained secure key rates. At the same time, possible choices are limited to observables that are accessible by the measurements Alice and Bob can carry out in their labs. For practical setups, this often will limit possible choices severely. We overcome this limitation by applying a matrix completion technique known from Refs. [10, 35] (see also Appendix A) to $r := \text{Re}(\rho_{AB})$ and

obtain $r_{j,l} \geq \frac{-r_{j,k}r_{k,l} - \sqrt{(r_{j,j}r_{k,k} - r_{j,k}^2)(r_{k,k}r_{l,l} - r_{k,l}^2)}}{r_{k,k}}$. Starting from density matrix entries that are known from (or at least bounded by) measurements, this allows us to iteratively obtain bounds on missing entries, extending the number of possible observables.

It remains to calculate the largest eigenvalue of M_ℓ , or bounds thereof, for a particular choice of observables. Strategies for upper-bounding or calculating eigenvalues heavily depend on the exact structure of M_ℓ , hence the choice of observables, and thus are highly problem-specific. Certain choices allow for a direct calculation with particular matrix structure-specific formulas, others can be tackled via generalized versions of the Sherman-Morrison formula, while some choices only allow for eigenvalue bounds, which introduce looseness in the obtained key rates but might simplify the problem further. For all those approaches, the optimisation problem then can be tackled using Lagrange's method, yielding quick results for the key rate at the cost of potentially lower key rates due to tailoring the observables for analytic solvability rather than maximal rates. Alternatively, one may pursue a semi-analytic approach, choosing observables with the goal of maximizing the key rate and solving for the largest eigenvalue numerically. This, however, means we require numerical optimisation for the solution of the optimisation problem in Eq. (2). Since each solution of the dual problem is a valid upper bound for the guessing probability by construction, this still leads to reliable lower bounds on the secure key rates. While this method is certainly more time-consuming than the purely analytical methods outlined earlier, it nevertheless reduces both computational complexity and time demands compared to direct numerical convex-optimisation approaches by far and opens the path to high dimensions, while still remaining flexible.

Demonstration and Results.— We illustrate our method for a high-dimensional temporal entanglement setup, analyzed earlier in Ref. [25] (Protocol 1), where a source prepares a d -dimensional state $|\Psi_1\rangle = |\text{DD}\rangle \otimes \frac{1}{\sqrt{d}} \sum_{k=0}^{d-1} |kk\rangle$ and Alice and Bob either measure the Time-of-Arrival (ToA), denoted as TT, or the temporal superposition of (not necessarily) neighboring time-bins (TSUP), denoted as SS. We obtain the following relations between the coincidence-click elements and density

matrix elements, $\text{TT}(i, j) = \langle i, j | \rho | i, j \rangle$ and

$$\text{Re}(\langle i, j | \rho^T | i-1, j-1 \rangle) = \frac{1}{4} \left(D(i, j, 0, 0) - D(i, j, \frac{\pi}{2}, \frac{\pi}{2}) \right), \quad (3)$$

$$\text{Re}(\langle i, j-1 | \rho^T | i-1, j \rangle) = \frac{1}{4} \left(D(i, j, 0, 0) + D(i, j, \frac{\pi}{2}, \frac{\pi}{2}) \right), \quad (4)$$

where $D(i, j, \phi^A, \phi^B)$ is a quantity derived from generalized x - and y -measurements, as elaborated on in Appendix B. This means by performing x , y , and z measurements, we have access to all diagonal elements and the real parts of certain off-diagonal elements. This can now be used to bound additional off-diagonal density matrix elements with the matrix completion technique mentioned earlier (see also Appendix A).

Inspired by entanglement witness theory [36, 37], and based on the measurements performed, we choose observables $\hat{W}_1 := q_0 \sum_{i=0}^{d-1} |i, i\rangle\langle i, i| + \sum_{z=1}^{d-1} \sum_{i=0}^{d-1} q_z (|i, i\rangle\langle i+z, i+z| + |i+z, i+z\rangle\langle i, i|)$ and $\hat{W}_2 := \sum_{i \neq j}^{d-1} p |i, j\rangle\langle i, j|$, where p and q_0, \dots, q_{d-1} are real numbers. While $w_2 := \text{Tr}[\rho_{AB} \hat{W}_2]$ is known with equality (at least in the asymptotic setting) from z -measurements, note that $w_1 := \text{Tr}[\rho_{AB} \hat{W}_1]$ is a function of diagonal elements and real parts of off-diagonal elements we can either measure directly or at least bound by the matrix completion technique. This, finally leads to the following optimization problem

$$\begin{aligned} & \min \gamma + S w_1^U + T w_2 \\ & \text{s.t.} \\ & \gamma \geq \lambda_{\max}(M_\ell) \quad \forall \ell = 0, \dots, d-1 \\ & S \in \mathbb{R} \\ & T \geq 0. \end{aligned} \quad (5)$$

We note that our choice of observables \hat{W}_1 and \hat{W}_2 leads to different dual variables appearing exclusively in orthogonal subspaces of M_ℓ , which simplifies the eigenvalue problem significantly. Our choice of observables used for this demonstration aims for high key rate rather than fastest possible evaluation, since some of the eigenvalues cannot be calculated analytically directly. Therefore, we split off those subspaces where analytic solutions are known and apply numerical methods to determine the largest eigenvalue of the remaining part each of the matrices M_ℓ rather than using eigenvalue bounds that introduce looseness. Then, we optimise the objective function numerically, emphasizing that we do not rely on finding the minimum exactly, as every found minimum upper-bounds the guessing probability by construction. In what follows we assume an isotropic noise model, $\rho = v |\Psi_1\rangle\langle\Psi_1| + \frac{(1-v)}{d^2} \mathbb{1}_{d^2}$, although we want to emphasize that this is only for demonstration purposes and our method does not rely on any particular noise model. We

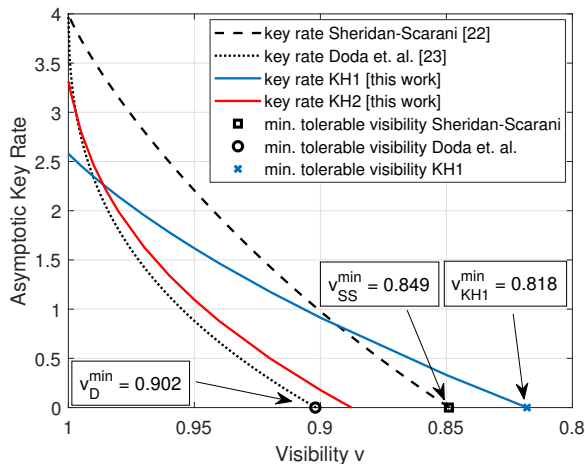


FIG. 1. Comparing key rates for $d = 16$ obtained with our method for two different operator choices, KH1 (blue) and KH2 (red), with rates obtained from the methods by Doda et. al. [23] (dotted black) and Sheridan-Scarani [22] (dashed black) for the same data. Our choice outperforms both in terms of maximal tolerable noise (minimal visibility v).

showcase our method for the high-dimensional QKD protocol discussed in Ref. [25] (see also Appendix B).

In Figure 1, we compare our method for two operator choices (see Appendix C for details) denoted by KH1 (solid blue) and KH2 (solid red) with secure key rates obtained by Ref. [23] (black dotted) and Ref. [22] (black dashed). While KH1 outperforms both in terms of maximal tolerable noise resistance (minimal tolerable visibility v), KH2 performs comparably to the results by Doda et. al. for high visibilities. This demonstrates the flexibility of or approach which allows choosing the operator based on the present noise level.

Next, we made a general operator Ansatz by choosing a parametrized exponential witness \tilde{W}_1 (see Appendix C) $q_z = e^{-c(z-s)}$, denoted KHexp, providing a two-parameter family of possible duals independent of system dimension. This already transcends the capabilities of SDP-based methods via opening up very high dimensions, concurrent with developments in experimental photonics [10, 18]. In Figure 2, we see that increasing dimension, with equal parameters c and s , already improves key rates across the entire range of visibilities and, moreover, increases noise resistance even without further subspace postselection, a feature not observed for Ref. [22] for limited measurement setups. When combining this Ansatz with the idea of subspace postselection QKD [23], we see that we can just as well harness the inherent noise resistance and dramatically decrease the visibility necessary for a positive key rate, while consistently outperforming the original subspace protocol.

All of this was achieved without extensive optimization of the witness choice, structure, and parameters p and q_z . Further improvement is possible with more in-depth optimization, facilitated by our flexible method that ac-

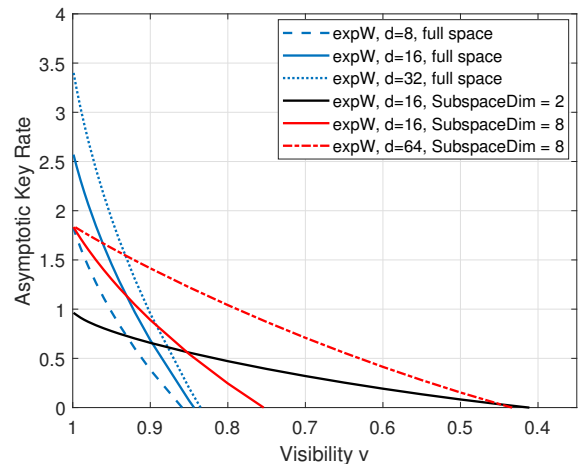


FIG. 2. Examination of secure key rates for different dimensions and different subspace postselection choices for KHexp with $c = 0.75$ and $s = 4$.

commodates a wide range of arbitrary observables and observable combinations. As this is not the main goal of this paper, maximizing key rates through witness optimization is left for future analysis of practical setups.

Discussion.— To summarise, we set out to overcome the constraints of high-dimensional QKD by unlocking high-dimensional protocols without the need for mutually unbiased measurements or SDP optimization. We derive a general framework based on analytic SDP duals for efficient key rate estimation and propose a family of witnesses suitable for time-bin or frequency-bin photonic setups. The speed of our method is basically dimension-independent, which unlocks high dimensions that remain inaccessible with numerical techniques. To our surprise, based on the same data, the operators employed for demonstration purposes already outperform standard techniques that have additional measurement capabilities and feature key rates comparable to the full SDP in dimensions where the latter is still computationally accessible. This was achieved without thorough witness optimization which hints that further improvement is possible. We believe that this solves a key critical issue in quantum communication, for the first time harnessing the full potential of genuinely high-dimensional entangled states in quantum key distribution with feasible measurement settings. The protocol considered for illustration is directly implementable in all higher-dimensional setups based on interfering neighboring bins, and we expect experimental demonstrations very soon. The obvious next step will be to go from asymptotic key rates to a finite key analysis, to which our min-entropy-based formulation is already very amendable.

ACKNOWLEDGMENTS

F.K. thanks Matej Pivoluska for fruitful discussions and precious feedback and Fabien Clivaz for enlightening discussions. This work has received funding from the



Horizon-Europe research and innovation programme under grant agreement No 101070168 (HyperSpace).

Appendix A: Matrix completion technique

In what follows, we briefly describe the matrix completion technique by Refs. [10, 35] and its application to our present problem.

A principle minor of M is $M_{I,J}$ where $I = J \subseteq \{1, \dots, n\}$. According to Sylvester's Criterion, every Hermitian $n \times n$ matrix M is positive semi-definite if and only if every nested sequence of principle minors has a non-negative determinant. Thus, in particular, if M is hermitian and positive semi-definite, $\det(M_{I,J}) \geq 0$ holds. This can be applied to the real part of a density matrix $r = \text{Re}(\rho) = (r_{i,j})_{i,j}$, which is positive semi-definite (as $r = \frac{1}{2}(\rho + \bar{\rho})$) and Hermitian (since symmetric). The condition that the determinant of every proper minor is non-negative, translates to

$$\det \begin{pmatrix} r_{j,j} & r_{j,k} & r_{j,l} \\ r_{k,j} & r_{k,k} & r_{k,l} \\ r_{l,j} & r_{l,k} & r_{l,l} \end{pmatrix} \geq 0 \Leftrightarrow r_{j,l} \geq \frac{r_{j,k}r_{k,l} \pm \sqrt{(r_{j,j}r_{k,k} - r_{j,k}^2)(r_{k,k}r_{l,l} - r_{k,l}^2)}}{r_{k,k}}. \quad (\text{A1})$$

Note that both $r_{j,j}r_{k,k} - r_{j,k}^2 \geq 0$ and $r_{k,k}r_{l,l} - r_{k,l}^2 \geq 0$ since both are the determinants of a 2×2 minor. Thus, the solution with minus is smaller than the solution using plus and we obtain

$$r_{j,l} \geq \frac{r_{j,k}r_{k,l} - \sqrt{(r_{j,j}r_{k,k} - r_{j,k}^2)(r_{k,k}r_{l,l} - r_{k,l}^2)}}{r_{k,k}}. \quad (\text{A2})$$

This relation can be used to iteratively derive lower bounds on the entries of r as needed to bound the expectation of the chosen observable. Thus, at the price of obtaining only bounds on the expectations instead of equalities, we can significantly extend the set of accessible observables.

Appendix B: Application to the HD temporal entanglement protocol

In this section, we detail the application of our method to the high-dimensional temporal entanglement protocol analysed in Ref. [25, Protocol 1], sticking close to the notation chosen there. In this protocol, a source prepares the state $|\Psi_{\text{target}}^{\text{P1}}\rangle := |\text{DD}\rangle \otimes \frac{1}{\sqrt{d}} \sum_{k=0}^{d-1} |kk\rangle$ which is distributed to Alice and Bob over the quantum channel. They then perform either a Time of Arrival (ToA) measurement or a Temporal Superposition (TSUP) measurement. We start with a brief recap of the most important definitions from [25]. The action of the temporal-superposition setup is described by

$$\begin{aligned} \hat{U} := & |\text{HH}\rangle\langle\text{HH}| \otimes \mathbb{1}_T \otimes \mathbb{1}_T + |\text{HV}\rangle\langle\text{HV}| \otimes \mathbb{1}_T \otimes \hat{Q}_\phi \hat{T} \\ & + |\text{VH}\rangle\langle\text{VH}| \otimes \hat{Q}_\phi \hat{T} \otimes \mathbb{1}_T + |\text{VV}\rangle\langle\text{VV}| \otimes \hat{Q}_\phi \hat{T} \otimes \hat{Q}_\phi \hat{T}. \end{aligned} \quad (\text{B1})$$

The TSUP measurement is then given by $\tilde{M}_{a,b}(i,j,\phi^A,\phi^B) := |\Psi_{a,b}(i,j,\phi^A,\phi^B)\rangle\langle\Psi_{a,b}(i,j,\phi^A,\phi^B)|$, where

$$|\tilde{\Psi}_{1,1}(i,j,\phi^A,\phi^B)\rangle := \hat{U}^\dagger |\text{DD}, i, j\rangle = |\tilde{\Psi}_1(i,\phi^A)\rangle \otimes |\tilde{\Psi}_1(j,\phi^B)\rangle, \quad (\text{B2})$$

$$|\tilde{\Psi}_{1,2}(i,j,\phi^A,\phi^B)\rangle := \hat{U}^\dagger |\text{DA}, i, j\rangle = |\tilde{\Psi}_1(i,\phi^A)\rangle \otimes |\tilde{\Psi}_2(j,\phi^B)\rangle, \quad (\text{B3})$$

$$|\tilde{\Psi}_{2,1}(i,j,\phi^A,\phi^B)\rangle := \hat{U}^\dagger |\text{AD}, i, j\rangle = |\tilde{\Psi}_2(i,\phi^A)\rangle \otimes |\tilde{\Psi}_1(j,\phi^B)\rangle, \quad (\text{B4})$$

$$\left| \tilde{\Psi}_{2,2}(i, j, \phi^A, \phi^B) \right\rangle := \hat{U}^\dagger |AA, i, j\rangle = \left| \tilde{\Psi}_2(i, \phi^A) \right\rangle \otimes \left| \tilde{\Psi}_2(j, \phi^B) \right\rangle, \quad (\text{B5})$$

and we introduced

$$\left| \tilde{\Psi}_x(i, \phi) \right\rangle := \frac{1}{\sqrt{2}} \left(|H, i\rangle + (-1)^{x-1} e^{-i\phi} |V, i-1\rangle \right), \quad (\text{B6})$$

for $x \in \{1, 2\}$. The ToA measurement is simply given by

$$M(i, j) := \mathbb{1}_{\text{Pol}} \otimes |i\rangle\langle i| \otimes |j\rangle\langle j|. \quad (\text{B7})$$

We denote ToA measurement clicks by $\text{TT}(i, j)$, while TSUP clicks are denoted by $\text{SS}_{a,b}(i, j, \phi^A, \phi^B)$, where the subscript denotes which of Alice's and Bob's detectors clicked.

It can be seen straight-forwardly that the ToA clicks directly give access to the diagonal elements of Alice's and Bob's shared density matrix ρ_{AB} . The action of the TSUP measurements read as follows,

$$\begin{aligned} 4\text{SS}_{1,1}(i, j, \phi^A, \phi^B) &= \text{Tr} \left[\tilde{M}_{1,1}(i, j, \phi^A, \phi^B) \rho_{AB} \right] \\ &= \langle i, j | \rho^T | i, j \rangle + \langle i, j-1 | \rho^T | i, j \rangle e^{-i\phi^B} \\ &\quad + \langle i-1, j | \rho^T | i, j \rangle e^{-i\phi^A} + \langle i-1, j-1 | \rho^T | i, j \rangle e^{-i(\phi^A + \phi^B)} \\ &\quad + \langle i, j | \rho^T | i, j-1 \rangle e^{i\phi^B} + \langle i, j-1 | \rho^T | i, j-1 \rangle \\ &\quad + \langle i-1, j | \rho^T | i, j-1 \rangle e^{i(\phi^B - \phi^A)} + \langle i-1, j-1 | \rho^T | i, j-1 \rangle e^{-i\phi^A} \\ &\quad + \langle i, j | \rho^T | i-1, j \rangle e^{i\phi^A} + \langle i, j-1 | \rho^T | i-1, j \rangle e^{i(\phi^A - \phi^B)} \\ &\quad + \langle i-1, j | \rho^T | i-1, j \rangle + \langle i-1, j-1 | \rho^T | i-1, j \rangle e^{-i\phi^B} \\ &\quad + \langle i, j | \rho^T | i-1, j-1 \rangle e^{i(\phi^A + \phi^B)} + \langle i, j-1 | \rho^T | i-1, j-1 \rangle e^{i\phi^A} \\ &\quad + \langle i-1, j | \rho^T | i-1, j-1 \rangle e^{i\phi^B} + \langle i-1, j-1 | \rho^T | i-1, j-1 \rangle \end{aligned} \quad (\text{B8})$$

$$\begin{aligned} 4\text{SS}_{1,2}(i, j, \phi^A, \phi^B) &= \text{Tr} \left[\tilde{M}_{1,2}(i, j, \phi^A, \phi^B) \rho_{AB} \right] \\ &= \langle i, j | \rho^T | i, j \rangle - \langle i, j-1 | \rho^T | i, j \rangle e^{-i\phi^B} \\ &\quad + \langle i-1, j | \rho^T | i, j \rangle e^{-i\phi^A} - \langle i-1, j-1 | \rho^T | i, j \rangle e^{-i(\phi^A + \phi^B)} \\ &\quad - \langle i, j | \rho^T | i, j-1 \rangle e^{i\phi^B} + \langle i, j-1 | \rho^T | i, j-1 \rangle \\ &\quad - \langle i-1, j | \rho^T | i, j-1 \rangle e^{i(\phi^B - \phi^A)} + \langle i-1, j-1 | \rho^T | i, j-1 \rangle e^{-i\phi^A} \\ &\quad + \langle i, j | \rho^T | i-1, j \rangle e^{i\phi^A} - \langle i, j-1 | \rho^T | i-1, j \rangle e^{i(\phi^A - \phi^B)} \\ &\quad + \langle i-1, j | \rho^T | i-1, j \rangle - \langle i-1, j-1 | \rho^T | i-1, j \rangle e^{-i\phi^B} \\ &\quad - \langle i, j | \rho^T | i-1, j-1 \rangle e^{i(\phi^A + \phi^B)} + \langle i, j-1 | \rho^T | i-1, j-1 \rangle e^{i\phi^A} \\ &\quad - \langle i-1, j | \rho^T | i-1, j-1 \rangle e^{i\phi^B} + \langle i-1, j-1 | \rho^T | i-1, j-1 \rangle, \end{aligned} \quad (\text{B9})$$

$$\begin{aligned}
4\text{SS}_{2,1}(i, j, \phi^A, \phi^B) &= \text{Tr} \left[\tilde{M}_{2,1}(i, j, \phi^A, \phi^B) \rho_{AB} \right] \\
&= \langle i, j | \rho^T | i, j \rangle + \langle i, j-1 | \rho^T | i, j \rangle e^{-i\phi^B} \\
&\quad - \langle i-1, j | \rho^T | i, j \rangle e^{-i\phi^A} - \langle i-1, j-1 | \rho^T | i, j \rangle e^{-i(\phi^A+\phi^B)} \\
&\quad + \langle i, j | \rho^T | i, j-1 \rangle e^{i\phi^B} + \langle i, j-1 | \rho^T | i, j-1 \rangle \\
&\quad - \langle i-1, j | \rho^T | i, j-1 \rangle e^{i(\phi^B-\phi^A)} - \langle i-1, j-1 | \rho^T | i, j-1 \rangle e^{-i\phi^A} \\
&\quad - \langle i, j | \rho^T | i-1, j \rangle e^{i\phi^A} - \langle i, j-1 | \rho^T | i-1, j \rangle e^{i(\phi^A-\phi^B)} \\
&\quad + \langle i-1, j | \rho^T | i-1, j \rangle + \langle i-1, j-1 | \rho^T | i-1, j \rangle e^{-i\phi^B} \\
&\quad - \langle i, j | \rho^T | i-1, j-1 \rangle e^{i(\phi^A+\phi^B)} - \langle i, j-1 | \rho^T | i-1, j-1 \rangle e^{i\phi^A} \\
&\quad + \langle i-1, j | \rho^T | i-1, j-1 \rangle e^{i\phi^B} + \langle i-1, j-1 | \rho^T | i-1, j-1 \rangle,
\end{aligned} \tag{B10}$$

$$\begin{aligned}
4\text{SS}_{2,2}(i, j, \phi^A, \phi^B) &= \text{Tr} \left[\tilde{M}_{2,2}(i, j, \phi^A, \phi^B) \rho_{AB} \right] \\
&= \langle i, j | \rho^T | i, j \rangle - \langle i, j-1 | \rho^T | i, j \rangle e^{-i\phi^B} \\
&\quad - \langle i-1, j | \rho^T | i, j \rangle e^{-i\phi^A} + \langle i-1, j-1 | \rho^T | i, j \rangle e^{-i(\phi^A+\phi^B)} \\
&\quad - \langle i, j | \rho^T | i, j-1 \rangle e^{i\phi^B} + \langle i, j-1 | \rho^T | i, j-1 \rangle \\
&\quad + \langle i-1, j | \rho^T | i, j-1 \rangle e^{i(\phi^B-\phi^A)} - \langle i-1, j-1 | \rho^T | i, j-1 \rangle e^{-i\phi^A} \\
&\quad - \langle i, j | \rho^T | i-1, j \rangle e^{i\phi^A} + \langle i, j-1 | \rho^T | i-1, j \rangle e^{i(\phi^A-\phi^B)} \\
&\quad + \langle i-1, j | \rho^T | i-1, j \rangle - \langle i-1, j-1 | \rho^T | i-1, j \rangle e^{-i\phi^B} \\
&\quad + \langle i, j | \rho^T | i-1, j-1 \rangle e^{i(\phi^A+\phi^B)} - \langle i, j-1 | \rho^T | i-1, j-1 \rangle e^{i\phi^A} \\
&\quad - \langle i-1, j | \rho^T | i-1, j-1 \rangle e^{i\phi^B} + \langle i-1, j-1 | \rho^T | i-1, j-1 \rangle.
\end{aligned} \tag{B11}$$

Now, we combine Eqs. (B8) - (B11) in the following way and obtain

$$\begin{aligned}
D(i, j, \phi^A, \phi^B) &:= \text{SS}_{1,1}(i, j, \phi^A, \phi^B) - \text{SS}_{2,2}(i, j, \phi^A, \phi^B) - \text{SS}_{2,1}(i, j, \phi^A, \phi^B) + \text{SS}_{2,2}(i, j, \phi^A, \phi^B) \\
&= e^{-i(\phi^A+\phi^B)} \langle i-1, j-1 | \rho_{AB} | i, j \rangle + e^{i(\phi^A-\phi^B)} \langle i, j-1 | \rho_{AB} | i-1, j \rangle \\
&\quad + e^{-i(\phi^A-\phi^B)} \langle i-1, j | \rho_{AB} | i, j-1 \rangle + e^{i(\phi^A+\phi^B)} \langle i, j | \rho_{AB} | i-1, j-1 \rangle.
\end{aligned}$$

Choosing $\phi_A = \phi_B = 0$ (corresponding to a generalized x measurement) yields

$$D(i, j, 0, 0) = 2 \text{Re} (\langle i, j-1 | \rho_{AB} | i-1, j \rangle) + 2 \text{Re} (\langle i, j | \rho_{AB} | i-1, j-1 \rangle), \tag{B12}$$

while for $\phi_A = \phi_B = \frac{\pi}{2}$ (corresponding to a generalized y measurement) leads to

$$D(i, j, \frac{\pi}{2}, \frac{\pi}{2}) = 2 \text{Re} (\langle i, j-1 | \rho_{AB} | i-1, j \rangle) - 2 \text{Re} (\langle i, j | \rho_{AB} | i-1, j-1 \rangle). \tag{B13}$$

Adding and subtracting Eqs. (B12) and (B13) respectively, yields

$$\text{Re} (\langle i, j | \rho^T | i-1, j-1 \rangle) = \frac{1}{4} \left(D(i, j, 0, 0) - D(i, j, \frac{\pi}{2}, \frac{\pi}{2}) \right), \tag{B14}$$

$$\text{Re} (\langle i, j-1 | \rho^T | i-1, j \rangle) = \frac{1}{4} \left(D(i, j, 0, 0) + D(i, j, \frac{\pi}{2}, \frac{\pi}{2}) \right). \tag{B15}$$

Thus, performing x - and y -measurements suffices to give us access to the real parts of certain off-diagonal elements. Note that in case we do only perform a generalized x -measurement, we can obtain at least a bound on the real parts of those off-diagonal elements,

$$\text{Re} (\langle i, j | \rho^T | i-1, j-1 \rangle) = \frac{D(i, j, 0, 0)}{4} - \sqrt{\text{TT}(i-1, j) - \text{TT}(i, j-1)}, \tag{B16}$$

which we can still use for our method.

Based on the obtained real parts, the method explained in Appendix A, allows us to iteratively bound additional off-diagonal elements.

Appendix C: Operator choices used for demonstration

In this section we state the choices made for the observables \hat{W}_1 and \hat{W}_2 used for KH1 and KH2 in Figures 1 and 2 in the main text. Recall that for demonstration purposes, we chose observables of the form $\hat{W}_1 := q_0 \sum_{i=0}^{d-1} |i, i\rangle\langle i, i| + \sum_{z=1}^{d-1} \sum_{i=0}^{d-1} q_z (|i, i\rangle\langle i+z, i+z| + |i+z, i+z\rangle\langle i, i|)$ and $\hat{W}_2 := \sum_{\substack{i,j=0 \\ i \neq j}}^{d-1} p |i, j\rangle\langle i, j|$, where p and q_0, \dots, q_{d-1} are chosen to be real numbers.

For KH1, we set $p = 1$ and for simplicity set $q_5 = \dots = q_{15} = 0$, while choosing $q_0 = -1$, $q_2 = 1$ and $q_3 = 2.7$ and $q_4 = 0.47$. For KH2, we set $p = 1$ and chose $q_0 = 0$, $q_1 = \dots = q_{11} = 1$ and $q_{12} = \dots = q_{15} = 0$. Finally, for the exponential witness KHexp, we chose, again $p = 1$ as well as $q_z = e^{-c(z-s)}$ for $c = 0.75$ and $s = 4$. To ease comparison, we kept those parameters fixed throughout the whole paper, despite dimension-dependent parameter choices would have increased key rates significantly in particular when subspace postselection was applied.

Both the choices of the form of \hat{W}_1 and \hat{W}_2 and the particular values inserted were solely for demonstration purposes and were not optimized systematically. Therefore, we expect different choices to lead to improved key rates for certain scenarios.

-
- [1] L. Han, Y. Li, P. Xu, X. Tao, W. Luo, W. Cai, S. Liao, and C. Peng, Integrated fabry–perot filter with wideband noise suppression for satellite-based daytime quantum key distribution, *Appl. Opt.* **61**, 812 (2022).
- [2] M. Abasifard, C. Cholsuk, R. G. Pousa, A. Kumar, A. Zand, T. Riel, D. K. L. Oi, and T. Vogl, The ideal wavelength for daylight free-space quantum key distribution (2023), arXiv:2303.02106 [quant-ph].
- [3] A. Krzic, D. Heinig, M. Goy, and F. Steinlechner, Dual-downlink quantum key distribution with entangled photons: prospects for daylight operation, in *International Conference on Space Optics — ICSO 2022*, Vol. 12777, edited by K. Minoglou, N. Karafolas, and B. Cugny, International Society for Optics and Photonics (SPIE, 2023) p. 1277726.
- [4] Y.-H. Li, S.-L. Li, X.-L. Hu, C. Jiang, Z.-W. Yu, W. Li, W.-Y. Liu, S.-K. Liao, J.-G. Ren, H. Li, L. You, Z. Wang, J. Yin, F. Xu, Q. Zhang, X.-B. Wang, Y. Cao, C.-Z. Peng, and J.-W. Pan, Free-space and fiber-integrated measurement-device-independent quantum key distribution under high background noise, *Phys. Rev. Lett.* **131**, 100802 (2023).
- [5] F. Bouchard, D. England, P. J. Bustard, K. L. Fenwick, E. Karimi, K. Heshami, and B. Sussman, Achieving ultimate noise tolerance in quantum communication, *Phys. Rev. Appl.* **15**, 024027 (2021).
- [6] M. Avesani, L. Calderaro, M. Schiavon, A. Stanco, C. Agnesi, A. Santamato, M. Zahidy, A. Scriminich, G. Folletto, G. Contestabile, M. Chiesa, D. Rotta, M. Artiglia, A. Montanaro, M. Romagnoli, V. Soriano, F. Vedovato, G. Vallone, and P. Villoresi, Full daylight quantum-key-distribution at 1550 nm enabled by integrated silicon photonics, *npj Quantum Information* **7**, 93 (2021).
- [7] S.-K. Liao, H.-L. Yong, C. Liu, G.-L. Shentu, D.-D. Li, J. Lin, H. Dai, S.-Q. Zhao, B. Li, J.-Y. Guan, W. Chen, Y.-H. Gong, Y. Li, Z.-H. Lin, G.-S. Pan, J. S. Pelc, M. M. Fejer, W.-Z. Zhang, W.-Y. Liu, J. Yin, J.-G. Ren, X.-B. Wang, Q. Zhang, C.-Z. Peng, and J.-W. Pan, Long-distance free-space quantum key distribution in daylight towards inter-satellite communication, *Nature Photonics* **11**, 10.1038/nphoton.2017.116 (2017).
- [8] P. G. Kwiat, Hyper-entangled states, *Journal of Modern Optics* **44**, 2173 (1997).
- [9] J. T. Barreiro, N. K. Langford, N. A. Peters, and P. G. Kwiat, Generation of hyperentangled photon pairs, *Phys. Rev. Lett.* **95**, 260501 (2005).
- [10] A. Martin, T. Guerreiro, A. Tiranov, S. Designolle, F. Fröwis, N. Brunner, M. Huber, and N. Gisin, Quantifying photonic high-dimensional entanglement, *Phys. Rev. Lett.* **118**, 110501 (2017).
- [11] N. T. Islam, C. C. W. Lim, C. Cahall, J. Kim, and D. J. Gauthier, Provably secure and high-rate quantum key distribution with time-bin qudits, *Science Advances* **3**, e1701491 (2017).
- [12] L. Bulla, M. Pivoluska, K. Hjorth, O. Kohout, J. Lang, S. Ecker, S. P. Neumann, J. Bittermann, R. Kindler, M. Huber, M. Bohmann, and R. Ursin, Nonlocal temporal interferometry for highly resilient free-space quantum communication, *Phys. Rev. X* **13**, 021001 (2023).
- [13] K. Sulimany, G. Pelc, R. Dudkiewicz, S. Korenblit, H. S. Eisenberg, Y. Bromberg, and M. Ben-Or, High-dimensional coherent one-way quantum key distribution (2023), arXiv:2105.04733 [quant-ph].
- [14] S. Ecker, F. Bouchard, L. Bulla, F. Brandt, O. Kohout, F. Steinlechner, R. Fickler, M. Malik, Y. Guryanova, R. Ursin, and M. Huber, Overcoming noise in entanglement distribution, *Phys. Rev. X* **9**, 041042 (2019).
- [15] J. Bavaresco, N. H. Valencia, C. Klöckl, M. Pivoluska, P. Erker, N. Friis, M. Malik, and M. Huber, Measurements in two bases are sufficient for certifying high-dimensional entanglement, *Nature Physics* **14**, 1032 (2018).
- [16] X.-M. Hu, W.-B. Xing, B.-H. Liu, Y.-F. Huang, C.-F. Li, G.-C. Guo, P. Erker, and M. Huber, Efficient generation of high-dimensional entanglement through multipath down-conversion, *Physical Review Letters* **125**, 10.1103/physrevlett.125.090503 (2020).
- [17] J. Schneeloch, C. C. Tison, M. L. Fanto, P. M. Alsing, and G. A. Howland, Quantifying entanglement in a 68-billion-dimensional quantum state space, *Nature Communications* **10**, 10.1038/s41467-019-10810-z (2019).
- [18] M. C. Ponce, A. L. M. Muniz, M. Huber, and F. Steinlechner, Unlocking the frequency domain for high-dimensional quantum information processing (2022), arXiv:2206.00969 [quant-ph].

- [19] A. S. Maxwell, L. B. Madsen, and M. Lewenstein, Entanglement of orbital angular momentum in non-sequential double ionization, *Nature Communications* **13**, 4706 (2022), publisher: Nature Publishing Group.
- [20] A. K. Sairam and C. M. Chandrashekar, Noise resilience in path-polarization hyperentangled probe states, *Journal of Physics B: Atomic, Molecular and Optical Physics* **55**, 225501 (2022).
- [21] P. A. A. Yasir and C. M. Chandrashekar, Generation of hyperentangled states and two-dimensional quantum walks using $\$J\$$ or $\$q\$$ plates and polarization beam splitters, *Physical Review A* **105**, 012417 (2022), publisher: American Physical Society.
- [22] L. Sheridan and V. Scarani, Security proof for quantum key distribution using qudit systems, *Physical Review A* **82**, 10.1103/physreva.82.030301 (2010).
- [23] M. Doda, M. Huber, G. Murta, M. Pivoluska, M. Plesch, and C. Vlachou, Quantum key distribution overcoming extreme noise: Simultaneous subspace coding using high-dimensional entanglement, *Physical Review Applied* **15**, 10.1103/physrevapplied.15.034003 (2021).
- [24] M. Araújo, M. Huber, M. Navascués, M. Pivoluska, and A. Tavakoli, Quantum key distribution rates from semidefinite programming, *Quantum* **7**, 1019 (2023).
- [25] A. Bergmayr, F. Kanitschar, M. Pivoluska, and M. Huber, How to harness high-dimensional temporal entanglement, using limited interferometry setups (2023), arXiv:2308.04422 [quant-ph].
- [26] P. J. Coles, E. M. Metodiev, and N. Lütkenhaus, Numerical approach for unstructured quantum key distribution, *Nat. Commun.* **7**, 11712 (2016).
- [27] A. Winick, N. Lütkenhaus, and P. J. Coles, Reliable numerical key rates for quantum key distribution, *Quantum* **2**, 77 (2018).
- [28] J. Lin, T. Upadhyaya, and N. Lütkenhaus, Asymptotic Security Analysis of Discrete-Modulated Continuous-Variable Quantum Key Distribution, *Phys. Rev. X* **9**, 041064 (2019).
- [29] F. Kanitschar and C. Pacher, Postselection Strategies for Continuous-Variable Quantum Key Distribution Protocols with Quadrature Phase-Shift Keying Modulation, arXiv:2104.09454v3 [quant-ph] (2021).
- [30] S. Bäuml, C. P. Garcia, V. Wright, O. Fawzi, and A. Acin, Security of discrete-modulated continuous-variable quantum key distribution (2023), arXiv:2303.09255 [quant-ph].
- [31] T. Upadhyaya, T. van Himbeek, J. Lin, and N. Lütkenhaus, Dimension Reduction in Quantum Key Distribution for Continuous- and Discrete-Variable Protocols, *PRX Quantum* **2**, 020325 (2021).
- [32] F. Kanitschar, I. George, J. Lin, T. Upadhyaya, and N. Lütkenhaus, Finite-size security for discrete-modulated continuous-variable quantum key distribution protocols, *PRX Quantum* **4**, 10.1103/prxquantum.4.040306 (2023).
- [33] I. Devetak and A. Winter, Distillation of secret key and entanglement from quantum states, *Proc. R. Soc. A* **461**, 207 (2005).
- [34] R. Renner and J. I. Cirac, de Finetti Representation Theorem for Infinite-Dimensional Quantum Systems and Applications to Quantum Cryptography, *Phys. Rev. Lett.* **102**, 110504 (2009).
- [35] A. Tiranov, S. Designolle, E. Z. Cruzeiro, J. Lavoie, N. Brunner, M. Afzelius, M. Huber, and N. Gisin, Quantification of multidimensional entanglement stored in a crystal, *Phys. Rev. A* **96**, 040303 (2017).
- [36] M. Huber and R. Sengupta, Witnessing genuine multipartite entanglement with positive maps, *Physical Review Letters* **113**, 10.1103/physrevlett.113.100501 (2014).
- [37] N. Friis, G. Vitagliano, M. Malik, and M. Huber, Entanglement certification from theory to experiment, *Nature Reviews Physics* **1**, 72–87 (2018).